ISBN: 978-3-95450-208-0 doi:10.18429/JACoW-IPAC2019-MOPMP039

DEVELOPMENTS IN THE EXPERIMENTAL INTERACTION REGIONS OF THE HIGH ENERGY LHC*

L. van Riesen-Haupt†, J.L. Abelleira, E. Cruz Alaniz, JAI, University of Oxford, Oxford, UK
J. Barranco, T. Pieloni, C. Tambasco, EPFL, Lausanne, Switzerland
M. Hofer, J. Keintzel, R. Tomás, F. Zimmermann, CERN, Geneva, Switzerland

Abstract

The High Energy LHC (HE-LHC) aims to collide 13.5 TeV protons in two high luminosity experiments and two low luminosity experiments. In the following, the recent updates in the two high luminosity experimental interaction regions (EIR) of the HE-LHC will be illustrated. In this update the β^* was increased from 0.25 m to 0.45 m to reduce beam-beam effects, while keeping the luminosity goal. On top of the triplet optics designed to achieve this, this paper will present energy deposition driven separation dipole designs, optics solutions for the matching section and dispersion suppressors as well as studies involving the integration into the lattice options. In particular it will outline geometric considerations as well as results from dynamic aperture studies.

INTRODUCTION

The Future Circular Collider (FCC) study [1] explores various accelerator options to succeed the Large Hadron Collider (LHC) and High Luminosity LHC (HL-LHC). One option aims to construct a hadron-hadron collider (FCC-hh) in an approximately 100 km circumference tunnel. By using novel Nb_3Sn technology to produce 16 T dipoles, the FCC-hh aims to reach a centre of mass (CoM) energy of 100 TeV. The High Energy LHC (HE-LHC) plans to use the same Nb_3Sn technology, but would be constructed in the 27 km LHC tunnel, resulting in a CoM energy of approximately 27 TeV [2]. An overview of the design parameters for the machines discussed above is shown in Table 1.

Table 1: Table Showing Various Machine Parameters for FCC-hh, HE-LHC and (HL-)LHC

Parameter	**FCC-hh**	**HE-LHC**	**(HL-)LHC**
C [km]	100	27	27
E_{beam} [TeV]	50	13.5	7
N $[\times 10^{11}]$	1	2.2	1.15 (2.2)
$\bar{\epsilon}$ [μm]	2.2	2.5	3.5 (2.5)
β^* [cm]	30	45	55 (15)
$\theta/2$ [μrad]	88	165	143 (250)
L $[\times 10^{34}\text{cm}^{-2}\text{s}^{-1}]$	30	28	1 (17)

The target energy of 27 TeV can not be reached by simply increasing the magnetic field of the LHC optics, but requires a careful redesign of the arcs to increase the filling factor whilst ensuring the machine fits in the LHC tunnel [3].

* Work supported by the Swiss institute for Accelerator Research and Technology , CHART.
† leon.vanriesen-haupt@physics.ox.ac.uk

Similarly, the optics of the interaction regions (IRs) in the eight straight sections have to be optimised to fulfil their purposes despite the more rigid beam. A first design of the two high luminosity experimental IRs (EIRs) was outlined in [4]. Since then the β^* was increased from 0.25 m to 0.45 m in order to achieve a more level luminosity evolution [5] and the crossing angle was increased from 12.5 σ to 16.8 σ to mitigate long range beam-beam effects. In the following the motivations for these changes and their impact on the design will be briefly discussed. In particular, this paper will look at the beam stay clear (BSC) in the triplet and at the dynamic aperture (DA) in the machine under these new conditions.

CROSSING ANGLE, β^* AND BEAM-BEAM EFFECTS

The strength of the long-range beam-beam effects defines the final choices on the crossing angle and the available aperture in the triplet for a defined β^*. This is evident looking at the beam to beam separation at the first encounter in the drift space defined as:

$$d_{sep} = \theta \cdot \sqrt{\beta^* \gamma / \epsilon_n}. \tag{1}$$

In order to establish satisfactory beam dynamics behaviour in the presence of beam-beam interactions, we follow the same criteria used for the design of the LHC [6] and the HL-LHC collision schemes [7], i.e. maintain a target value of the DA around 6 σ for the HE-LHC emittance of 2.5 μm in the presence of the beam-beam effects and no magnetic errors. Based on LHC experience and studies [8, 9] and experimental observations, this choice avoids the appearance of chaotic motion with associated losses and emittance deterioration [10]. For the HE-LHC a beam-beam separation of approximately 17 σ is needed to ensure a DA of approximately 6.0 σ as shown in Fig. 1 where the DA is shown as a function of d_{sep} for the nominal intensity (the blue line) and for slightly lower values (the red and green lines). This separation will ensure a good control of the beam-beam long range effects at all stages of the collider operational cycle. Figure 1 clearly indicates that the impact of a normalised separation of 12.5 σ, as initially foreseen, would be too severe for safe operation. This larger crossing angle becomes feasible since an increased β^* operation at 45 cm is proposed in order to get a more level luminosity evolution [11]. This allows increasing the normalized separation from 12.5 to 16.8 σ while keeping the crossing angle at 330 μrad, as can be easily deduced from Eq.1. This implies that the required crab cavity voltage remains unchanged and the energy deposition studies from the previous iteration remain valid [12].

ISBN: 978-3-95450-208-0 doi:10.18429/JACoW-IPAC2019-MOPMP039

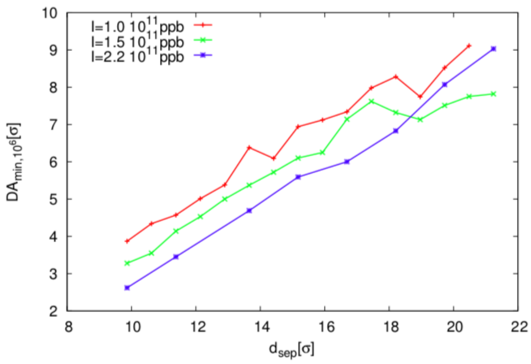

Figure 1: One-million turn DA as a function of the beam to beam normalized separation for the nominal intensity (blue) and lower values (green and red).

The strong radiation damping at 13.5 TeV beam energy helps to increase the margins on the DA and it can be used to account for other non-linearities such as the magnets imperfections, high chromaticity operation and Landau octupoles needed for stability. Detailed studies are needed to define the minimal separation required while the intensities decay during collision. The crossing angle might be further decreased if beam-beam compensation techniques are studied and applied [13, 14].

BEAM STAY CLEAR

For low β^* values, the β-functions in triplet can be approximated to vary proportional to $1/\beta^*$. Therefore, since the absolute crossing angle at the IP is kept the same and the β^* is increased compared to the previous design, the BSC in the triplet should increase. To test this, the β^* is re-matched using the EIR matching section and the BSC in the triplet and separation dipoles is computed using MAD-X [15]. The computation assumes the default MADX parameters that are based on the LHC. These include a β beating factor of 20 %, fractional parasitic dispersion of 0.273, a beam halo of 6 σ, orbit tolerances of 2 mm and a momentum spread of 2×10^{-4}. The resulting optics and BSC are shown in Fig. 2.

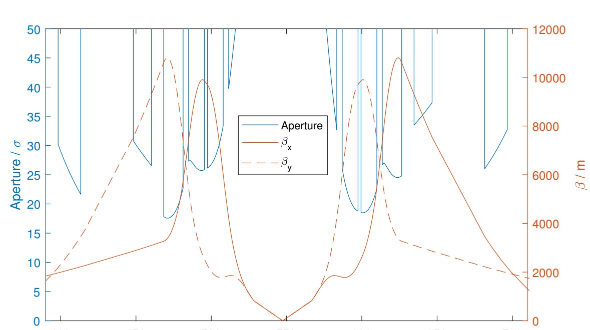

Figure 2: β-functions and BSC in HE-LHC triplet and separation dipoles for $\beta^* = 0.45$ m.

Figure 2 shows that the minimum BSC of the triplet is about 17.5 σ, which is, as expected, significantly above the 12.5 σ required. This gives a comfortable margin to reach lower β^* values, which might be required if the luminosity is lower than expected. The additional BSC can also be used to further increase the crossing angle if needed, however, this would increase the crab cavity voltage required and has an impact on the luminosity. The BSC is calculated in separation dipoles as detailed in Table 2, with an inner, single aperture separation dipole (D1) with an 80 mm coil radius and an outer separation dipole (D2) with two coil apertures with radii of 38.5 mm. It should be noted that no shielding is assumed in the dipoles for the BSC computation.

Table 2: Parameters of the Separation Dipoles

	D1	D2
Aperture	Single	Double
Length [m]	12	15
Dipole field [T]	9.68	7.75
Aperture radius [mm]	55	26
Coil radius [mm]	80	38.5

MATCHING

As before, the matching section is based on the matching section of the LHC with some magnets increased in length in order to have enough integrated strength for the more rigid beam whilst not exceeding the maximum gradient of 360 T/m. The matching section can sufficiently match the 0.45 m β^* whilst ensuring the EIR matches the arc at the interface. The limitation of this matching remains that the vertical phase advance to the first sextupole on the left of the EIR cannot be optimally matched for spurious dispersion correction [16]. The matching section can also be used to achieve an injection optics with an 11 m β^*, which provides sufficient BSC at injection as presented in [4].

ENERGY DEPOSITION IN DIPOLES

Since the absolute crossing angle and triplet magnet strength remain unchanged from the previous design and the integrated lifetime luminosity is still assumed to be 10 ab^{-1}, the energy deposition in the triplet remains unchanged and is still below 30 MGy as required [12]. At the same time, the peak power density decreases since the peak luminosity is decreased.

From the results of the BSC studies, the maximum allowed uniform shielding in D1 and D2 can be calculated. For D1 this results in 21.5 mm of shielding whilst D2 can only accommodate 9 mm of uniform shielding. Dipoles with these design and shielding parameters were added to the FLUKA [17] model to study the dose over the HE-LHC's lifetime, the results for D1 and D2 are shown in Fig. 3 and Fig. 4 respectively. Whilst the lifetime dose in D1 is well below the 30 MGy threshold, Fig. 4 shows that the dose in D2 is too high when using 9 mm of uniform shielding.

ISBN: 978-3-95450-208-0 doi:10.18429/JACoW-IPAC2019-MOPMP039

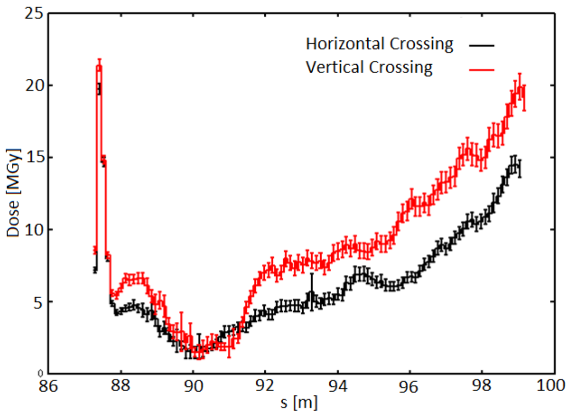

Figure 3: Radiation dose deposited in HE-LHC D1 over a $10\,\mathrm{ab}^{-1}$ lifetime.

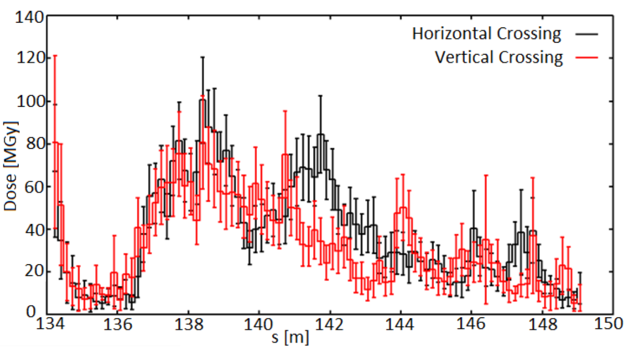

Figure 4: Radiation dose deposited in HE-LHC D2 over a $10\,\mathrm{ab}^{-1}$ lifetime.

One solution to this problem may be the use of non-uniform shielding that is shaped to match the trajectory of the beam along the dipole as shown in Fig. 5. In such a scenario, the shielding can be varied from 9 mm to 27 mm. First results from simulations performed with such a configuration have shown that this can reduce the dose in D2 to below 40 MGy, which is much closer to the acceptable limit.

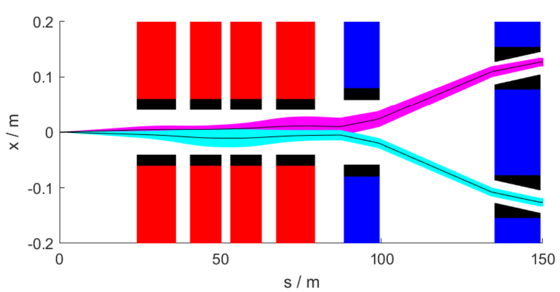

Figure 5: Horizontal beam trajectories through triplet quadrupoles (red) and separation dipoles (blue) with shielding (black) in HE-LHC EIR.

DYNAMIC APERTURE

The final aspect of the EIR that needs to be explored is the impact these changes have on the DA when triplet errors are implemented but without beam-beam effects. To this end, triplet errors, scaled from the HL-LHC triplet error table [7] are applied to the lattice before it is converted for tracking in SixTrack [18]. The tracking is performed using 10^6 turns and 60 random number seeds to generate the errors and is evaluated at seven angles. Like for the BSC, the closed-orbit uncertainty of 2 mm was also used but a momentum spread of 1.7×10^{-4} was used, based on predictions of the RF system [19].

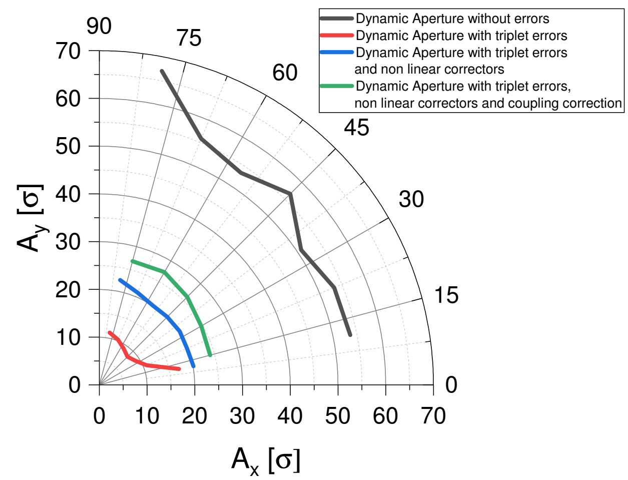

Figure 6: DA evaluated for HE-LHC with and without triplet errors and with correction schemes.

Tracking is performed for various scenarios and the results are interpreted using the SixDesk software [20] and are shown in Fig. 6. As seen in Fig. 6, when triplet errors are applied, the DA reduces from $50\,\sigma$ to $8\,\sigma$. Based on experiences in the LHC [21] and FCC-hh [22], a simulated DA with triplet errors of about $15-20\,\sigma$ would be required for stable operation. In order to achieve this goal, the non-linear corrector package installed behind D2 was set to cancel the $c(a_3;0,3)$ and $c(a_3;3,0)$ as well as the $c(b_3;1,2)$ and $c(b_3;2,1)$ resonance driving terms as described in [23]. This increases the DA to $20\,\sigma$, as seen in Fig. 6, the DA can be further increased to $24\,\sigma$ by implementing the double tuning scheme used in FCC-hh [22]. This DA is more than sufficient for operation and significantly larger than for the previous case [4], this is mainly due to the lower β-functions in the triplet, resulting in lower resonance driving terms.

CONCLUSION

It has been shown that the proposed changes in β^* and crossing angle with respect to the first iteration of the EIR design have a positive impact on the DA due to both beam-beam effects and non-linear triplet errors. The changes ensure that the DA is in an acceptable regime whilst having little to no impact on other design aspects. The current design also includes a realistic separation scheme that is shown to have adequate shielding.

ISBN: 978-3-95450-208-0 doi:10.18429/JACoW-IPAC2019-MOPMP039

REFERENCES

[1] FCC, https://fcc-cdr.web.cern.ch/.

[2] M. Benedikt *et al.*, "Future Circular Collider: Conceptual Design Report Vol. 3" CERN-ACC-2018-0058, accepted for publication in EPJ ST, 2018.

[3] J. Keintzel *et al.*, “HE-LHC Optics Design Options”, presented at the 10th Int. Particle Accelerator Conf. (IPAC’19), Melbourne, Australia, May 2019, paper MOPMP026, this conference.

[4] L. van Riesen-Haupt *et al.*, “Experimental Interaction Region Optics for the High Energy LHC”, in *Proc. 9th Int. Particle Accelerator Conf. (IPAC’18)*, Vancouver, Canada, Apr.-May 2018, pp. 360–363. doi:10.18429/JACoW-IPAC2018-MOPMK006

[5] F. Zimmermann *et al.*, “Updated High-Energy LHC Design”, presented at the 10th Int. Particle Accelerator Conf. (IPAC’19), Melbourne, Australia, May 2019, paper MOPMP037, this conference.

[6] W. Herr *et al.*, Long range beam-beam effects, in *Proc. ICFA Mini-Workshop on Beam-Beam Effects in Hadron Colliders*, CERN, Geneva, Switzerland, 18-22 Mar. 2013.

[7] G. Apollinari *et al.*, "High-Luminosity Large Hadron Collider (HL-LHC) : Technical Design Report V. 0.1", in *CERN Yellow Reports: Monographs*, Geneva, Switzerland, Apr. 2017.

[8] T. Pieloni *et al.*, Two beam effects, in *Proc. 5th Evian Workshop on LHC beam operation*, CERN-ACC-2014-0319(2014), pp. 69-79, Evian, France, 2–4 Jun. 2014.

[9] T. Pieloni *et al.*, Beam-beam effects long-range and head-on, in *Proc. 6th Evian Workshop on LHC beam operation*, CERN-ACC-2015-376, pp. 111-122, Evian, France, Jun. 2014.

[10] M. P. Crouch *et al.*, “Dynamic Aperture Studies of the Long-Range Beam-Beam Interaction at the LHC”, in *Proc. 8th Int. Particle Accelerator Conf. (IPAC’17)*, Copenhagen, Denmark, May 2017, pp. 3840–3843. doi:10.18429/JACoW-IPAC2017-THPAB056

[11] F. Bordry *et al.*, "Machine Parameters and Projected Luminosity Performance of Proposed Future Colliders at CERN" arXiv:1810.13022, CERN-ACC-2018-0037, 2018.

[12] J. L. Abelleira, E. Cruz Alaniz, A. Seryi, and L. van Riesen-Haupt, “HE-LHC Final Focus: Flat Beam Parameters and Energy Deposition Studies”, in *Proc. 9th Int. Particle Accelerator Conf. (IPAC’18)*, Vancouver, Canada, Apr.-May 2018, pp. 356–359. doi:10.18429/JACoW-IPAC2018-MOPMK005

[13] J. P. Koutchouk, Principle of a Correction of the Long-Range Beam-Beam Effect in LHC using Electromagnetic Lenses, LHC-Project-Note 223, Geneva, Switzerland, 2000.

[14] V. D. Shiltsev, Electron lenses for Super Colliders, New York, NY, USA: Springer 2016, pp. 95-135.

[15] MAD-X, http://MAD-X.web.cern.ch/MAD-X/

[16] L.H.A. Leunissen, "Influence of vertical dispersion and crossing angle on the performance of the LHC", CERN-LHC-Project-Report-298, Geneva, Switzerland, 1999.

[17] FLUKA, http://www.fluka.org/

[18] SixTrack, http://sixtrack.web.cern.ch/SixTrack/

[19] E. Shaposhnikova, HE-LHC: Longitudinal beam parameters. Geneva, Switzerland, Jul 2018. HE-LHC General Design Meeting.

[20] E. McIntosh, R. De Maria, " The SixDesk Run Environment for SixTrack", CERN-ATS-Note-2012-089, Geneva, Switzerland, 2018.

[21] J.-P. Koutchouk, "The LHC dynamic aperture", in *Proc. PAC’99*, New York, NY, USA, Mar. 1999.

[22] E. Cruz Alaniz, J. L. Abelleira, A. Seryi, L. van Riesen-Haupt, R. Martin, and R. Tomas, “Methods to Increase the Dynamic Aperture of the FCC-hh Lattice”, in *Proc. 9th Int. Particle Accelerator Conf. (IPAC’18)*, Vancouver, Canada, Apr.-May 2018, pp. 3593–3596. doi:10.18429/JACoW-IPAC2018-THPAK145

[23] O.S. Brüning *et al.*, "Dynamic Aperture Studies for the LHC Separation Dipoles", CERN-LHC-Project-Note-349, Geneva, Switzerland, 2004.